Bandpass Signal Sampling and Coherent Detection

Coherent detectors in radar and communications receivers are generally implemented in the form of two parallel baseband channels which form in-phase (I) and quadrature (Q) components of a received RF/IF signal. Phase errors of several degrees due to imperfect matching of these separate channels limit the performance achievable from signal processors such as moving target indicators (MTI), coherent integrators, Doppler filters, antenna array processors, and coherent sidelobe cancellers.

Thus methods in which a single analog to digital (A/D) converter samples and digitizes the IF signal directly, eliminating the need for IF to baseband conversion, have been of recent interest and are the subject of this paper. To obtain accurate coherent detection from IF samples taken near the Nyquist rate requires interpolation based upon a number of stored samples. An algorithm derived from sampling theory is defined and used to demonstrate accurate reconstruction of the original IF signal from digitized samples. In-phase and quadrature components of the signal are shown to be available from processed samples with demonstrated phase errors less than 0.2°.

INTRODUCTION

Radar and communications systems are becoming increasingly dependent upon coherent digital processing. Conversion of signals from IF analog form into digital complex samples carrying phase and amplitude information has been traditionally implemented in the form of two parallel IF to baseband converters operated in quadrature each followed by A/D converters which thus provide digitized in-phase (I) and quadrature (Q) components (Fig. 1). Balancing the two baseband converters over a wide dynamic range is difficult and phase errors are typically 2°-3° for commercial coherent detectors [1]. Fig. 2 represents the general approach to bandpass signal sampling of interest here. A digital processor provides in-phase and quadrature components I_n and Q_n from samples taken directly from the original signal. This approach requires only one A/D converter and is shown to provide improved accuracy (phase errors less than 0.2°).

CALCULATION OF I AND Q FROM IF SAMPLES

Any bandpass signal $r(t)$ may be written

$$\begin{aligned} r(t) &= A(t)\cos[2\pi f_0 t + \phi(t)] \\ &= A(t)\cos\phi(t)\cos 2\pi f_0 t \\ &\quad - A(t)\sin\phi(t)\sin 2\pi f_0 t \end{aligned}$$

Manuscript received December 29, 1981; revised May 25, 1982.

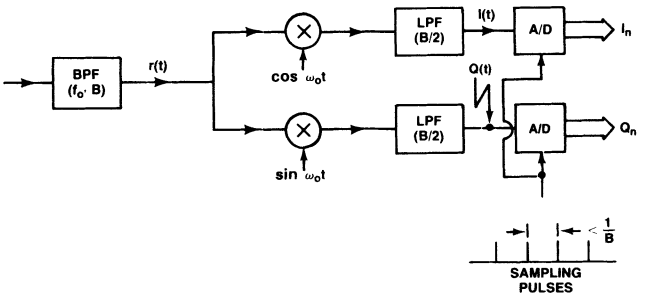

Fig. 1. Conventional approach to coherent detection.

$$= I(t)\cos 2\pi f_0 t - Q(t)\sin 2\pi f_0 t \qquad (1)$$

where f_0 is the center frequency of the passband B (Figs. 1 and 2). Equation (1) implicitly defines quantities $A(t)$, $\phi(t)$, $I(t)$, and $Q(t)$ conventionally referred to as signal amplitude, phase, in-phase component, and quadrature component, respectively.

Fig. 3 illustrates the digital processing called for in Fig. 2. The analog to digital converter (A/D) provides digitized values sampled from $r(t)$ at a rate $2W > 2B$. A finite impulse response (FIR) digital filter stores $2N + 1$ of these samples in a shift register and computes a value $r(t_n - N/2W + {}^1/_4 f_0')$ according to (2) for each n (f_0' is defined later and n identifies a digitized sample). $2N + 1$ values of $r(t_n)$ are weighted and combined to compute $\hat{r}(t_n - N/2W + {}^1/_4 f_0') = \hat{r}(t_m + {}^1/_4 f_0')$.

Pairs of values (A, B, C, and D in Fig. 3) are selected by the two four-position switches to provide pairs of in-phase and quadrature samples, I_m and Q_m. The corresponding selection rule is discussed below.

$$\hat{r}(t) = \sum_{-N+J(t)}^{+N+J(t)} r(n/2W)s(t - n/2W) \qquad (2)$$

where the general problem of interpolation from sampled values is discussed in Appendix A; interpolation functions $s(t)$ are discussed in Appendix B. $J(t) = \mathrm{Int}(t + {}^1/_4 W)$ and Int(x) equals the largest integer less than or equal to x.

The need for interpolating to form the estimates of I_m and Q_m is illustrated by (3), which may be derived from (1), making the substitution $f_0 = (2M-1)W/2$, where M is any integer. The effect of this choice of f_0 in relation to the sample rate $2W$ is to make each sampled value (see (3)) a sample of either I or Q depending on whether $m = n + N$ is even or odd.

$$\begin{aligned} r(t_m) &= (-1)^{m/2} I(t_m), \qquad m \text{ even} \\ &= (-1)^{(m-1)/2} Q(t_m), \qquad m \text{ odd}. \end{aligned} \qquad (3)$$

It is tempting to define a coherent detector based only upon (3) since alternate samples are equal to samples of I and Q. This is legitimate if A and ϕ in (1) are constant. However we are usually interested in values of $A(t)$ and $\phi(t)$, where both vary with time. Ideally we need samples of I and Q taken at the same instant.

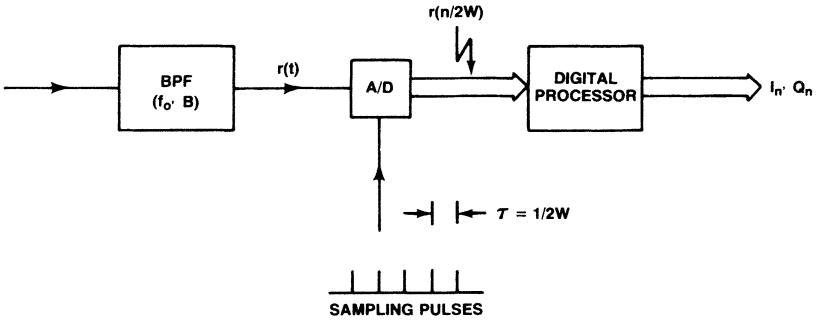

Fig. 2. Direct sampling and digital coherent detection.

As long as $f_0 >> W$ (large M), we may write

$$\hat{r}(t_m + \frac{1}{4f_0}) = -(-1)^{m/2}\hat{Q}(t_m + \frac{1}{4f_0})$$
$$\simeq -(-1)^{m/2}Q(t_m), \qquad m \text{ even}$$
$$= (-1)^{(m-1)/2}\hat{I}(t_m + \frac{1}{4f_0})$$
$$\simeq (-1)^{(m-1)/2}I(t_m), \qquad m \text{ odd}. \qquad (4)$$

However we want f_0, the carrier frequency of the sampled IF signal, to be small enough to avoid A/D converter aperture errors. Thus we take advantage of the fact that $r_m' = r_m$, where $r'(t)$ is given by (1) with f_0 replaced by $f_0' = [(2M' - 1)/2]\,W$, where M' is an integer.

That is, a bandpass time function $r'(t)$ having a different (higher) carrier frequency but with the same sampled values $r_m' = r_m$ is defined by judicious choice of carrier frequencies and sampling rate. Hence, making $f_0' >> f_0$ arbitrarily large, we may write

$$\lim_{f_0' \to \infty} \hat{r}(t_m + {}^1/_4 f_0') = (-1)^{m/2}\,\hat{Q}(t_m), \qquad m \text{ even}$$
$$= (-1)^{(m-1)/2}\,\hat{I}(t_m),$$
$$m \text{ odd}. \qquad (5)$$

Thus $\hat{r}(t_m + {}^1/_4 f_0')$ approaches corresponding values of I and Q with arbitrarily small error as long as $\hat{r}$ is a good estimate of r. The matter of accurate interpolation is treated in Appendix B.

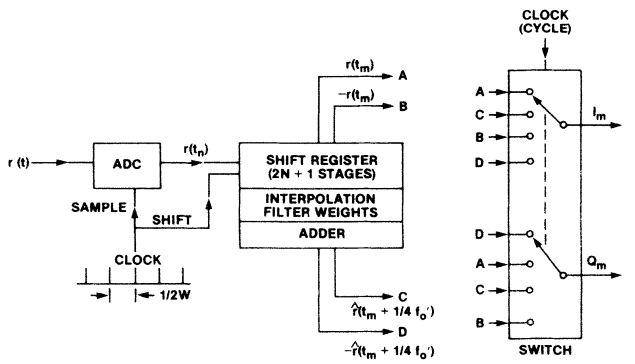

Fig. 3. Digital coherent detector.

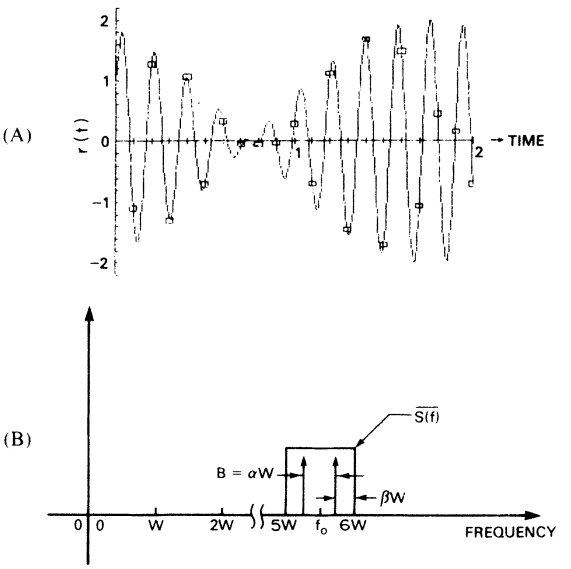

Fig. 4. (A) Continuous wave test signal waveform and (B) spectrum. (□ points are computed values of $M = 6$, $\alpha = 0.5$, $\beta = 0.25$.)

INTERPOLATION AND PHASE ERROR CALCULATIONS

Two classes of waveforms were employed in testing the accuracy of coherent detector algorithms. The dual sine wave signal (Fig. 4) was most useful, as both phase and amplitude variations are present when their frequencies are asymmetrically located in the band. A Gaussian pulse modulating a sine wave was also used to examine the effects of spectral energy outside the limits $(M-1)W \leq f \leq MW$. Fig. 5 shows Gaussian pulse waveforms and interpolation error for two pulse widths τ. The pulse is given by $r(t) = \exp[-(t/\tau)^2/2]$. Note that the short-pulse interpolation errors exceed the longer pulse errors by about one order of magnitude.

Early results using the truncated cardinal series (Appendix A) revealed truncation errors in interpolation and corresponding phase errors which are plotted in Fig. 6 for the dual sine wave, where bandwidth B, normalized to the Nyquist complex sample rate W, is varied. Note that even for 2:1 oversampling rms errors reach nearly 2°.

Later studies led to an improved interpolation algorithm based upon a "self-truncating" sampling function discussed in Appendix B. Fig. 11 contains graphs of in-

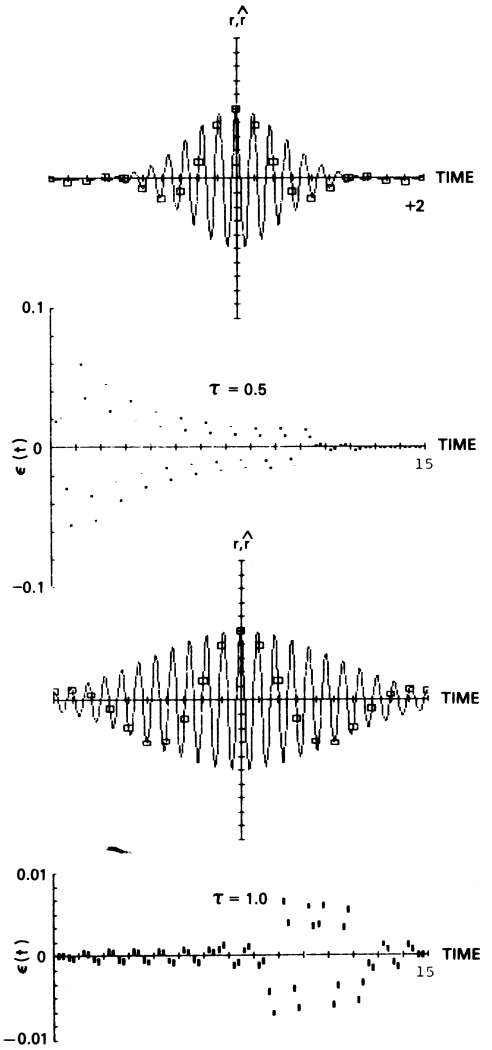

Fig. 5. Waveforms and interpolation errors for sine waves (f_0 = 5.5 W) modulated by two Gaussian pulses (truncated cardinal series; see Appendix A).

terpolation error (an upper bound derived for the low-pass case) comparing the self-truncating algorithm with the standard sin x/x form. Errors are plotted against N, where $2N + 1$ is the number of stored samples upon which the interpolation is based. Note that the error bound corresponding to the self-truncating algorithm falls with increasing N at a much faster rate than that of the cardinal series. For this reason we extended self-truncating interpolation to the bandpass case and applied it to the coherent detector algorithm.

Results are presented in Fig. 7 in which coherent detector phase errors (peak and rms) are plotted against normalized bandwidth, where a self-truncating algorithm was used for interpolation. Note that, relative to Fig. 6, phase errors have been reduced by more than an order of magnitude over the range from 0 to 0.5 corresponding to 2:1 oversampling. In the example considered in Figs. 6 and 7, the sine wave frequencies were symmetrically located in the band from $5W$ to $6W$, resulting in a composite phase which is constant for half the modulation cycle changing by 180° as the envelope goes through zero and remaining constant until the envelope again passes through zero.

However in the example of Fig. 8 the frequencies were chosen equal to $5.3W$ and $5.8W$, giving rise to a changing phase as well as changing amplitude. Signal phase varies from 139.5° to 112.5° over the four samples located at t = 1, 1.5, 2.0, and 2.5; note that phase estimates remained accurate with errors between + 0.058° and −0.066° over this range.

SUMMARY AND CONCLUSIONS

We have described a method whereby a single A/D converter operating in conjunction with appropriate processing produces I and Q components of a narrow-band signal for each sample point. An algorithm based upon the sampling theorem was tested in software using CW and pulsed waveforms demonstrating the accuracy of the process. Tests of the detector with a self-truncating interpolation algorithm produced peak phase errors less than 0.2°, an order of magnitude better than is available from conventional baseband detectors. Experiments with an off the shelf A/D converter (Computer Labs Model 7105) reveal that accurate samples are obtained at a 2.5-MHz rate

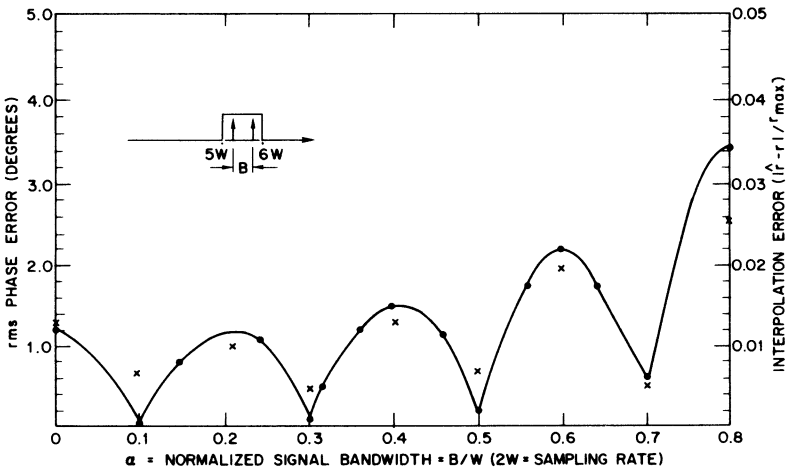

Fig. 6. Direct sampling coherent detector phase error (.) and interpolation error (x) using cardinal series interpolation.

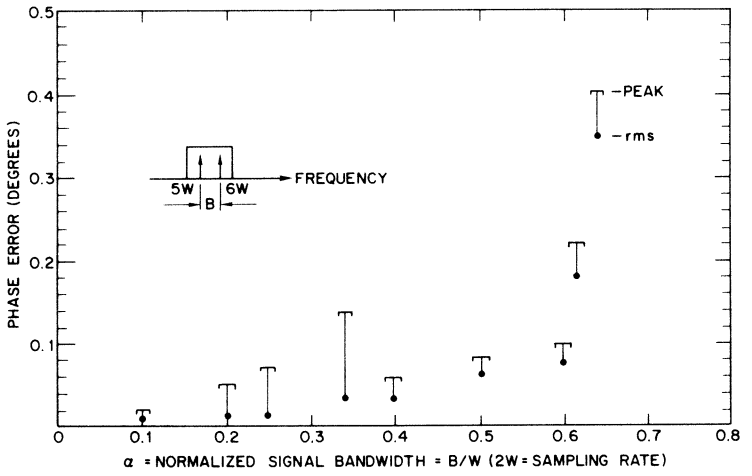

Fig. 7. Peak and rms errors in phase estimated using self-truncating interpolation algorithm.

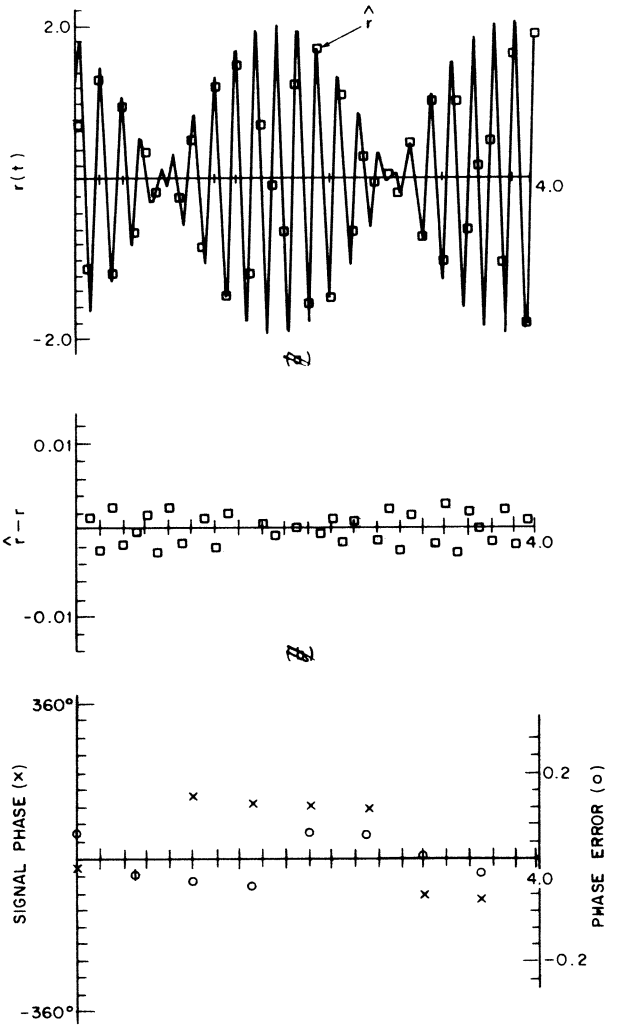

Fig. 8. (A) Test signal $r(t)$ plotted with points interpolated from values sampled at 0, 0.5, 1.0, ...; (B) interpolation error, $\hat{r} - r$; (C) signal phase computed from same samples plotted with phase estimation error.

from sine waves at frequencies well above the converter sampling rate (up to 20 MHz). The converter tested is rated at 5-MHz maximum sampling rate. New converters projected by various manufacturers are expected to be capable of extending this limit by an order of magnitude to accommodate higher IF frequencies.

The impact of more accurate coherent detection should appear in improved digital pulse compression sidelobe levels, MTI cancellation ratios, and antenna array processing. Cost is a factor but future LSI convolver devices [2] should make direct sampling methods of the type described here less expensive as well as more accurate than conventional detectors.

APPENDIX A

LOW-PASS AND BANDPASS SAMPLING FUNCTIONS

If we define a signal $r(t)$ to have no spectral energy beyond a limit W, it is well known that all information about the signal is contained in a sequence of samples taken at a uniform rate greater than $2W$. Stated in another way, the original signal $r(t)$ may be exactly reconstructed by an interpolation

$$r(t) = \sum_n r(n/2W)s(t - n/2W) \tag{A1}$$

where the sampling (interpolation) function

$$s(t) = \frac{\sin(2\pi Wt)}{2\pi Wt} \tag{A2}$$

is the well known cardinal function. Note that $s(t)$ is of the form $\sin x/x$; its transform is a spectral "window" function of height $1/2W$ and width $2W$, centered about zero.

These well known statements of the Nyquist theorem facilitate the statement of a similar theorem for bandpass signals. Equation (A1) also holds for signals with frequency spectra confined to two bands of width W symmetrically located about zero extending between MW and $(M - 1)W$ for $f > 0$ and $-MW$, $-(M - 1)W$ for $f < 0$, where M is any positive integer, and where the sampling function $s(t)$ may be found from the corresponding spectral "window" function.

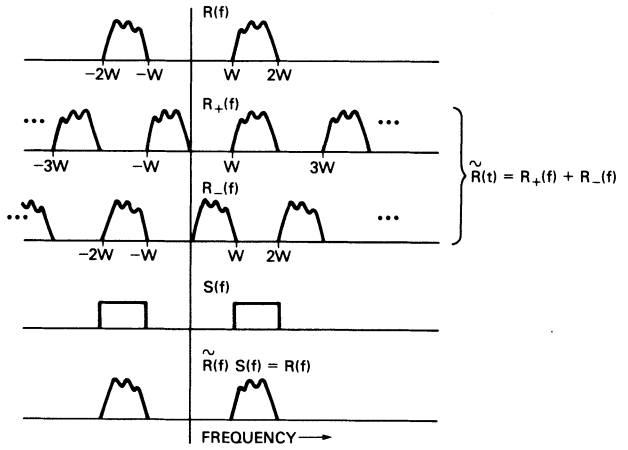

Fig. 9. Spectra of signal $R(f)$, samples signal, $\hat{R}(f)$, interpolation function $S(f)$, and the reconstructed signal $R(f)S(f)$.

A bandpass window may be formed from two low-pass windows (2) extending from $-MW$ to $+MW$ and $-(M-1)W$ to $+(M-1)W$. Subtracting the latter from the former and taking the transform we have, for the bandpass case,

$$s(t) = \frac{\sin 2\pi MWt - \sin 2\pi(M-1)t}{2\pi Wt}. \tag{A3}$$

Fig. 9 illustrates bandpass sampling and reconstruction. M must be an integer since the process of sampling causes duplication of both positive and negative frequencies; otherwise contributions from positive and negative parts of $R(f)$ overlap thus preventing the window function $S(f)$ (interpolation filter) from recovering the original signal $r(t)$. This is evident by inspection of Fig. 9. Note the last line of the figure (identical to the first) is $R(f)$, the spectrum of the original signal $r(t)$. An example of $s(t)$ where $M = 2$ is shown in Fig. 10.

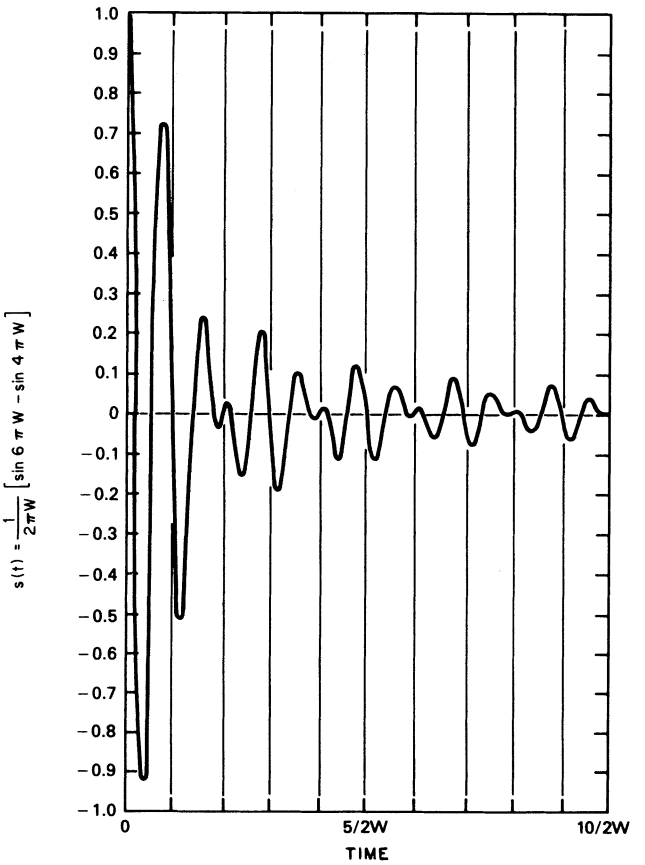

Fig. 10. Graph of bandpass interpolation function $s(t)$; $M = 3$.

APPENDIX B

REDUCTION OF TRUNCATION ERRORS IN BANDPASS SIGNAL INTERPOLATION

Appendix A states that a signal $r(t)$ may be exactly recovered from samples according to (A1) involving a summation over infinite limits. In practice we are restricted to an algorithm with finite limits. Specifically, the coherent detector involves the summation of (2) containing $2N + 1$ terms which provides $\hat{r}(t)$, an estimate of $r(t)$, from the samples $r(n/2W)$.

Helms and Thomas [7] investigated the effect of changing the sampling function $s(t)$ upon the estimation error and found that by replacing the cardinal functions given by (A3) by

$$s(t) = \left\{ \frac{[\sin 2\pi(q/p)Wt]}{2\pi(q/p)Wt} \right\}^p \cdot \frac{\sin 2\pi MWt - \sin 2\pi(M-1)Wt}{2\pi Wt} \tag{B1}$$

where $q = 1 - B/W$ and $p = \mathrm{Int}(Nq\pi/e)$, the error is considerably reduced. e is the base of the natural logarithm.

Fig. 11 contains curves of an upper bound on interpolation error versus N for two cases involving the cardinal

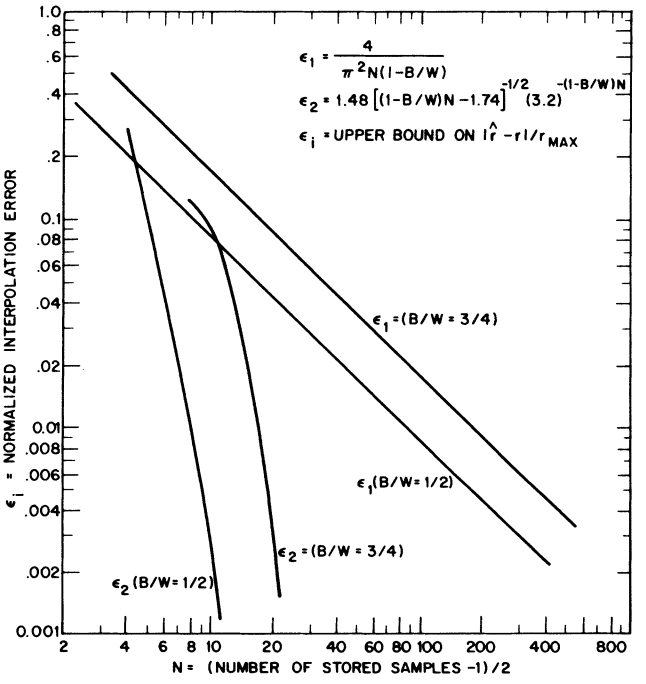

Fig. 11. Cardinal series (ϵ_1) and self-truncating interpolation (ϵ_2) error bounds as a function of truncation length (N).

function of (A3) and the "self-truncating" function above. These were plotted from relationships derived in reference [7]. Note the substantial error reduction achieved by the self-truncating form of $s(t)$.

W.M. WATERS

B.R. JARRETT

Radar Division
Naval Research Laboratory
Washington, D.C. 20375

REFERENCES

[1] Merrimac Industries (1980)
Signal processing components and subsystems.
1980 Merrimac Industries Catalogue, Merrimac Industries, PCM-3 Series Phase Comparator, p. 13, 1980.

[2] Waters, W.M., and Jarrett, B.R. (1980)
Bandpass signal sampling and coherent processing.
Report 8520, Naval Research Lab., Washington, D.C., Nov. 1980.

[3] Linden, D.A. (1959)
A discussion of sampling theorems.
Proceedings of the IRE, July 1959.

[4] Kohlenberg, A. (1953)
Exact interpolation of bandlimited functions.
Journal of Applied Physics, 1953, *24*, 1432-1436.

[5] ITT Handbook (1977)
Reference Data for Radio Engineers.
New York: Howard Sams and Co., 1977.

[6] Panter, P.F. (1965)
Modulation, Noise, and Spectral Analysis.
New York: McGraw-Hill, 1965.

[7] Helms, H.D., and Thomas, J.B. (1962)
Truncation error sampling theorem expansions.
Proceedings of the IRE, 1962, *50*, 179-184.

Quadrature Sampling With High Dynamic Range

Many radio and sonar systems require signal outputs in complex low-pass form. To achieve this, it is possible to use uniform sampling of the bandpass signal, together with computation of the quadrature component by way of a Hilbert transform. The bandpass to low-pass translation is accomplished by undersampling. A hardware implementation is described which achieves 70 dB spurious-free dynamic range and a bandwidth of 30 kHz.

I. INTRODUCTION

There are a number of radio and sonar applications in which it is convenient or necessary that the sensor output signals be translated to a complex low-pass (in-phase and quadrature) representation. Examples of applications which require the processing of signals in this form are sampled-aperture arrays [1], adaptive beamforming arrays [2], and the holographic radio camera [3]. The processing of acoustic signals from hydrophone arrays may also use this approach [4].

The processing of signals in quadrature low-pass form is founded on the so-called analytic signal representation [5], whereby signals are in general treated as complex exponentials rather than as purely real functions. The low-pass case is a specialization of the more general topic of sampling of bandpass signals, which has received considerable attention [6-10].

Quadrature low-pass signals may be obtained in a number of ways. A conventional method, shown in Fig. 1, involves a pair of analog multipliers or mixers, in which the received signal, at some convenient center frequency, is multiplied by a reference signal of frequency equal to the center frequency. The output is then low-pass filtered. A 90° phase shift is imposed in one of the channels in either the signal or reference path, so that the resulting outputs from the multipliers are in-phase quadrature. A second method, second order sampling, avoids some of the limitations of the analog multiplier method by sampling the signal directly in sample pairs, the samples comprising each pair being spaced in time by $^1/_4$ period of the midband frequency [7, 9]. (More generally, the pair spacing may be $N+(^1/_4)$ periods, where N is an integer.) In some cases, it may be necessary to compensate for various errors which arise in hardware implementations of quadrature detectors [11].

In this correspondence, we describe hardware which provides a simple solution to the problem of bandpass sampling. It achieves high dynamic range and requires sampling at or above the Nyquist rate as determined by the signal bandwidth, not by the highest frequency component of the bandpass signal. By properly choosing the sampling frequency in relation to the center frequency and bandwidth, the frequency-domain periodic-repetition property of the discrete Fourier transform is exploited in such a way that the low-pass complex signal is obtained with little computational effort. The bandpass signal is sampled at uniform intervals, and the quadrature component is computed via a digital Hilbert transform [12, 13].

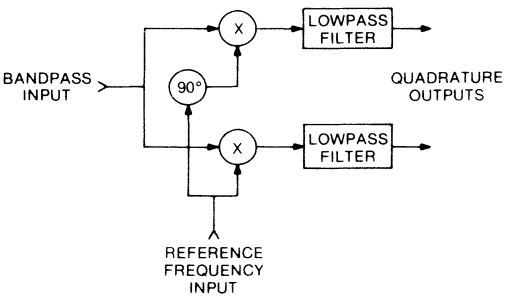

Fig. 1. Conventional quadrature detection technique, using analog multipliers (X).

Manuscript received April 1, 1982.

This work was supported by the Program for Industry/Laboratory Projects of the Government of Canada. The design and implementation of this work were undertaken at Miller Communications Systems Ltd., 300 Legget Dr., Kanata, Ont., Canada, K2K 1Y5.